0026-895X/02/6203-473–484$7.00
MOLECULAR PHARMACOLOGY
Copyright © 2002 The American Society for Pharmacology and Experimental Therapeutics
*Mol Pharmacol* 62:473–484, 2002

Vol. 62, No. 3
1607/1003843
*Printed in U.S.A.*



# Glutamate Cascade to cAMP Response Element-Binding Protein Phosphorylation in Cultured Striatal Neurons through Calcium-Coupled Group I Metabotropic Glutamate Receptors

LIMIN MAO and JOHN Q. WANG

*Department of Pharmacology, School of Pharmacy, University of Missouri-Kansas City, Kansas City, Missouri*

Received January 14, 2002; accepted May 24, 2002

This article is available online at http://molpharm.aspetjournals.org

## ABSTRACT

Emerging evidence indicates that group I metabotropic glutamate receptors (mGluRs) play a significant role in the addictive plasticity of striatal neurons. The plasticity is probably mediated by altered cellular gene expression in relation to stimulation of group I mGluRs and associative signaling proteins. In this study, we investigated the signaling linkage of surface group I mGluRs to the nuclear transcription factor cAMP response element-binding protein (CREB) in cultured primary striatal neurons. We found that selective activation of group I mGluRs (primarily the mGluR5 subtype) was able to up-regulate CREB phosphorylation in neurochemically identified γ-aminobutyratergic neurons but not glia. The CREB phosphorylation was independent of kainate/AMPA receptors but partially dependent of concomitant NMDA receptor activation. Because L-type voltage-operated $Ca^{2+}$ channel inhibitors substantially blocked the CREB phosphorylation, group I receptors are believed to lead to activation of L-type $Ca^{2+}$ channels, resulting in the CREB phosphorylation. Indeed, further studies on signaling pathways showed that group I mGluRs, by activating phospholipase C, induced a rapid and transient $Ca^{2+}$ release from the 1,4,5-triphosphate-sensitive rather than ryanodine-sensitive $Ca^{2+}$ store. The transient $Ca^{2+}$ rise in turn triggered the opening of L-type $Ca^{2+}$ channels, resulting in a progressively larger increase in cytoplasmic $Ca^{2+}$ levels that is responsible for subsequent CREB phosphorylation. These results indicate that $Ca^{2+}$-coupled group I mGluRs possess the ability to up-regulate CREB phosphorylation via the intracellular $Ca^{2+}$ release-induced activation of L-type $Ca^{2+}$ channels and, to a lesser extent, NMDA receptors in primary striatal neurons.

Metabotropic glutamate receptors (mGluRs) are referred to as G-protein-coupled receptors. Through G-proteins, eight subtypes of mGluRs are linked to different second messenger systems (Kendall, 1993; Nakanishi and Masu, 1994). Group I mGluRs (mGluR1/5 subtypes) are demonstrated to mainly affect intracellular $Ca^{2+}$ mobilization (Conn and Pin, 1997; Bordi and Ugolini, 1999). To sequentially facilitate intracellular $Ca^{2+}$ ($[Ca^{2+}]_i$) release, group I receptors activate the membrane-bound phospholipase C (PLC), which stimulates phosphoinositide turnover by hydrolyzing phosphoinositol-4,5-biphosphate to 1,4,5-triphosphate ($IP_3$) and diacylglycerol. $IP_3$ then causes the release of $Ca^{2+}$ from intracellular $Ca^{2+}$ stores (such as endoplasmic reticulum) by binding to specific $IP_3$ receptors on the membrane of $Ca^{2+}$ stores (Berridge, 1993). Altered $Ca^{2+}$ levels could then engage in the modulation of broad cellular activities.

MGluR1/5 receptors are densely expressed in the medium-sized spiny projection neurons of striatum (Fotuhi et al., 1993; Shigemoto et al., 1993; Testa et al., 1995; Kerner et al., 1997; Tallaksen-Greene et al., 1998). With recently available agonists and antagonists relatively selective for the group I receptor, functional roles of this subgroup of glutamate receptors in the regulation of striatal functions are being discovered rapidly. For example, striatal group I receptors are found to regulate motor activity. Enhanced local receptor activity by intrastriatal injection of a group I agonist, 3,5-

This work was supported by National Institutes of Health Grants R01-DA10355 and R01-MH61469 and a University of Missouri Research Board grant from the University of Missouri (all to J.Q.W.).

**ABBREVIATIONS:** mGluR, metabotropic glutamate receptor; aCSF, artificial cerebrospinal fluid; AMPA, (*S*)-α-amino-3-hydroxy-5-methyle-4-isoxazole propionic acid; AP5, DL-2-amino-5-phosphonovaleric acid; CPCCOet, 7-(hydroxyimino)cyclopropa[b]chromen-1*a*-carboxylate ethyl ester; CREB, cAMP response element-binding protein; DHPG, 3,5-dihydroxyphenylglycine; DMSO, dimethyl sulfoxide; FPL64176, 2,5-dimethyl-4-[2-(phenylmethyl)benzoyl]-1*H*-pyrrole-3-carboxylic acid methylester; $IP_3$, 1,4,5-triphosphate; MAP2, microtubule-associated protein-2a + 2b; MPEP, 2-methyl-6-(phenylethynyl)pyridine hydrochloride; MSOPPE, (*R*,*S*)-α-methylserine-O-phosphate monophenyl ester; PBS, phosphate-buffered saline; PHCCC, *N*-phenyl-7-(hydroxyimino)cyclopropa[b]chromen-1*a*-carboxamide; PLC, phospholipase C; VOCC, voltage-operated $Ca^{2+}$ channel; NeuN, neuronal nuclear antigen; GABA, γ-aminobutyric acid; MK801, dizocilpine maleate; NMDA, *N*-methyl-D-aspartate; DNQX, 2,3-dihydroxy-6,7-dinitroquinoxaline; U73122, 1-[6-[[17β-methoxyestra-1,3,5(10)-trien-17-yl]amino]hexyl]-1*H*-pyrrole-2,5-dione; U73343, 1-[6-[[17β-3-methoxyestra-1,3,5(10)-trien-17-yl]amino]hexyl]-2,5-pyrrolidine-dione.

dihydroxyphenylglycine (DHPG), caused contraversive turning (Kearney et al., 1997) or long-lasting locomotion and stereotypical behavior (Mao and Wang, 2000; Wang and Mao, 2000). Besides motor stimulation, DHPG up-regulated prodynorphin and proenkephalin mRNA expression in striatal neurons both in vivo (Mao and Wang, 2001a) and in vitro (Mao and Wang, 2001b). This group I-regulated gene expression has been suggested to play a crucial role in the development of neuroplasticity related to the addictive properties of drugs of abuse or other striatal disorders (Wang and Mao, 1999; Wang et al., 2002).

The group I regulation of gene expression may be mediated via the transcription factor cAMP response element-binding protein (CREB). Through binding to the promoter $Ca^{2+}$ and cAMP response element, phosphorylated CREB (pCREB) relays to transmit the extracellular signal conveyed through the surface receptor and its associative signaling pathways to target DNA transcription (Bito et al., 1996; Silva et al., 1998). To date, the CREB-regulated transcription has been linked to a variety of normal and abnormal neural activities, including memory and learning in hippocampal neurons (Bourtchuladze et al., 1994; Yin et al., 1994; Segal and Murphy, 1998; Silva et al., 1998) and addictive neuroplasticity in striatal neurons (Nestler et al., 1993; Konradi et al., 1994; Simpson et al., 1995; Rajadhyaksha et al., 1998). Both $Ca^{2+}$ and cAMP are the principal second messengers controlling the phosphorylation of CREB at its regulatory site, $Ser^{133}$ (Montminy et al., 1990; Bito et al., 1996; Hardingham et al., 1997; Johnson et al., 1997). As demonstrated consistently in cultured hippocampal and striatal neurons, elevated $Ca^{2+}$ influx through glutamate activation of $Ca^{2+}$-permeable NMDA or (*S*)-α-amino-3-hydroxy-5-methyle-4-isoxazole propionic acid (AMPA) receptors increased the phosphorylation of CREB (Bading et al., 1993; Ghosh and Greenberg, 1995; Das et al., 1997; Perkinton et al., 1999; Schurov et al., 1999; Choe and McGinty, 2000; Hardingham et al., 2001). Similarly, $Ca^{2+}$ entry through L-type voltage-operated $Ca^{2+}$ channels (VOCCs) led to increased CREB phosphorylation (Greenberg et al., 1992; Rajadhyaksha et al., 1999; Dolmetsch et al., 2001). However, up to now, no attempt has been made to define the regulatory role of group I mGluR subtypes and $[Ca^{2+}]_i$ release in CREB phosphorylation.

The present study was therefore designed to characterize the phosphorylation of CREB by the $Ca^{2+}$-coupled group I mGluRs in striatal neurons. A well characterized striatal culture model was used in which >90% of cells are GABAergic neurons, and the vast majority of those neurons express mGluR1 and mGluR5 receptors (Mao and Wang, 2001b). We found that activation of group I mGluRs led to the robust phosphorylation of CREB in cultured striatal neurons. This inducible phosphorylation was mediated via $Ca^{2+}$ release-induced $Ca^{2+}$ influx involving L-type VOCC and NMDA receptor activation.

## Materials and Methods

**Primary Striatal Neuronal Cultures.** The standardized procedure for the primary striatal neuronal culture preparation in this laboratory (Mao and Wang, 2001b) was employed in the present study. Briefly, the E19 rat embryos or neonatal 1-day-old rat pups (Charles River Laboratories, Inc., Wilmington, MA) were decapitated, and brains were rapidly removed and placed in a petri dish half-filled with cold sterile 1× PBS (~0.145 M). The striata were dissected out under a dissecting microscope and placed into another dish containing ice-cold PBS to thoroughly remove blood vessels and membrane from striatal tissues. The tissues were incubated in 0.25% trypsin (Invitrogen, Carlsbad, CA) for 20 min at 37°C for proteolytic digestion, followed by centrifuge for 2 min at 800 rpm. Dissociation of cells was achieved by gentle trituration through fire-narrowed Pasteur pipettes in PBS containing bovine serum albumin (1 mg/ml), DNase I (10 μg/ml), and soybean trypsin inhibitor (0.5 mg/ml). After centrifugation for 5 min at 1000 rpm, cells were resuspended in Dulbecco's modified Eagle's medium/Ham's F12 medium containing 10% fetal bovine serum (Invitrogen), 1× B27 (Invitrogen), 10 g/L glucose (Sigma-Aldrich, St. Louis, MO), 10 mg/L gentamicin (Invitrogen), and 10 mg/L penicillin/streptomycin (Invitrogen) and counted on a hemocytometer using Trypan Blue. The cellular death, as assessed by Trypan Blue exclusion, was less than 5%, and an average yield was approximately 0.9 to $1.2 \times 10^6$ cells per neonate. Cells were diluted to a final concentration of $3 \times 10^5$ cells/ml, and 0.5 ml per chamber was plated onto 0.01% poly-D-lysine-coated removable eight-chamber glass slides (for immunocytochemistry) or cover glasses (extra thin for fluorescent $Ca^{2+}$ detection). Cultures were incubated at 37°C in 5% $CO_2$ and 100% humidity. After 24 h, the medium was replaced by a fresh mixture of 70% Dulbecco's modified Eagle's medium/Ham's F12 medium and 30% neurobasal (Invitrogen). The medium was changed every 5 to 7 days, and 5 μM 1-β-D-arabinofuransylcytosine (Sigma-Aldrich) was added on day 4 and remained at this concentration in the medium before use to control the proliferation of nonneuronal cells. Cells were usually cultured for 18 to 20 days before use unless otherwise indicated. Using the procedures mentioned above, a predominant GABA-ergic neuronal culture has been demonstrated, as evidenced by the fact that >90% of total cells were immunoreactive to glutamic acid decarboxylase-65/67, GABA, or the specific marker for neurons (microtubule-associated protein-2a + 2b, MAP2) but not for glia (glial fibrillary acidic protein) (Mao and Wang, 2001b).

**Immunocytochemistry.** The indirect ABC immunocytochemistry on slides was performed as described previously (Choe and Wang, 2001; Mao and Wang, 2001b) to detect pCREB immunoreactivity in cultured cells. Briefly, cultures were fixed in 4% paraformaldehyde for 10 min, followed by 10-min incubation with 1% Triton X-100. To block nonspecific staining, cultures were incubated with 4% normal horse serum (universal VECTASTAIN Elite ABC Kit; Vector Laboratories, Burlingame, CA) and 1% bovine serum albumin (Vector Laboratories) for 20 min. Rabbit polyclonal antisera against CREB or pCREB (Cell Signaling Technology Inc., Beverly, MA) were used as primary antibodies and diluted 1:2000 with 1% normal horse serum. The cells were treated with primary antibodies overnight at 4°C and incubated with biotinylated secondary antibody (horse anti-rabbit IgG, 1:200; Vector Laboratories) for 1 h at room temperature before incubation with avidin-biotin-horseradish peroxidase complex (Vector Laboratories) for 1 h. Finally, 3,3′-diaminobenzidine (0.25 mg/ml with 0.01% $H_2O_2$) containing an intensifier 0.04% nickel chloride was used as a chromagen (for 4–6 min).

Double immunofluorescent labeling was performed to phenotype the cells expressing pCREB. Cultures were blocked by normal donkey serum and incubated overnight at 4°C in a mixture of two primary antibodies: rabbit anti-pCREB (1:250–500) with mouse anti-MAP2 (1:500; Chemicon International, Temecula, CA), mouse anti-neuronal nuclear antigen (NeuN; 1:500; Chemicon International), or mouse anti-GABA (1:250–500; Sigma-Aldrich). After several rinses in 1× PBS, sections were incubated for 1 h with donkey secondary antibodies (1:200) conjugated to CY3 (anti-rabbit IgG) or CY2 (anti-mouse IgG) from Jackson Immunoresearch Laboratories, Inc. (West Grove, PA). Sections were then rinsed and mounted in anti-fade medium (Vectashield; Vector Laboratories). For both single and double labeling, omittance of the primary antibodies served as negative controls.

**Quantitative Analysis of pCREB Immunoreactivity.** Because the immunocytochemical reaction and staining density may vary from time to time, all drug-treated and control wells in a study were processed simultaneously with the same batch of reagents. Images were acquired via a Fluor 10× objective and a charge-coupled device video camera (Sony XC-77; Sony Corp., Tokyo, Japan) coupled to a Nikon E800 microscope (Tokyo, Japan) and transferred onto a computer monitor in a TIFF-format National Institutes of Health image to improve visualization and to sample image in one focal plane. Cell counting was performed in each well by a person unaware of the treatment protocol. Both positive and negative cells were counted on the basis of a clearly visible pCREB-labeled (obviously different from the background) or unlabeled nucleus, respectively. Cells with ambiguous labeling or an unidentifiable nucleus were excluded from analysis. Neurons and astrocytes were counted separately. Phenotypes of neuronal and astrocytic cells were easily identified according to their morphological characteristics. Neurons showed small (8–12 $\mu$m) or medium-sized (13–19 $\mu$m), phase-bright cell bodies with branching processes, whereas astrocytes were large and flat with phase-dark, large pale nuclei (25–35 $\mu$m) and abundant and widely spread cytoplasms (Mao and Wang, 2001b). The unidentifiable phenotype of cells was not counted. Five optic fields per well (one at the center and four approximately at ~1.5 mm from the four edges of the well; 800 × 800-$\mu$m each) were selected for cell counting. The total number of neurons in one optic field usually ranged from 100 to 180. The pCREB-positive cells were calculated as the percentage of total cells per optic field. The percentages of five optic fields were averaged as a mean for a well and treated as $n = 1$. For double immunofluorescent analysis, immunostaining was first examined under a Nikon E800 dual epifluorescence microscope with a 40× oil objective. Confirmation of double labeling was then achieved using a confocal microscope with a 60× objective. To obtain the proportion of pCREB-immunoreactive cells that were neurons or GABA-ergic neurons, 50 to 100 pCREB-positive cells per well were analyzed to evaluate the percentage of pCREB cells immunoreactive for the specific neuronal markers (MAP2 or NeuN) or GABA. Images were imported into Photoshop (Adobe Systems Inc., Mountain View, CA) for composition purposes.

**Single-Cell $[Ca^{2+}]_i$ Measurements and $[Ca^{2+}]_i$ Imaging.** The culture was loaded with artificial cerebrospinal fluid (aCSF) (123 mM NaCl, 0.86 mM $CaCl_2$, 3.0 mM KCl, 0.89 mM $MgCl_2$, 25 mM $Na_2HCO_3$, 0.50 mM $NaH_2PO_4$, and 0.25 mM $Na_2HPO_4$ aerated with 95% $O_2$/5% $CO_2$, pH 7.4) containing 3 $\mu$M fura-2/acetoxymethyl ester (Sigma-Aldrich). After a 40-min incubation at 37°C, cultures were thoroughly rinsed with aCSF lacking fura-2/acetoxymethyl ester to remove unincorporated fluorescent particles. Cultures were allowed to sit at room temperature for 30 min for complete de-esterification. When required, cultures were bathed in aCSF solution with no added $Ca^{2+}$ and supplemented with 100 $\mu$M EGTA, referred to as $Ca^{2+}$-free solution. Under a Nikon TE300 inverted epifluorescence microscope with a 75-W xenon arc lamp, the fluorescence of cytosolic fura-2 was sequentially excited at 340 and 380 nm through an oil immersion objective (40×) via a dichroic mirror. A spinning filter wheel shutter controller (Lambda 10-2; Sutter Instrument Co., Novato, CA) controlled band-pass filters of 340 and 380 nm, which are installed in front of the xenon lamp to illuminate specimens with two excitation beams alternatively. Emitted light was collected from the sample through a dichroic mirror and a 510-nm bandpass filter and directed to a cooled, intensified charge-coupled device video camera (IC-110; Photon Technology International, Monmouth Junction, NJ). The fluorescent signal was measured at a single neuronal cell, which can be readily identified by its phase-bright appearance (Mao and Wang, 2001b). $Ca^{2+}$ digital recordings are made from the cell soma. Image pairs were captured approximately every 6 s. Baseline was recorded for 3 to 5 min before bath application of drugs. The $[Ca^{2+}]_i$ response to drug treatments was usually monitored continuously for 30 min, to which most evoked $[Ca^{2+}]_i$ responses were confined. Background measurements were always automatically subtracted from cellular signals.

The $[Ca^{2+}]_i$ concentration was calculated from ratios of the intensities of emitted fluorescence at two excitation wavelengths ($F_{340}/F_{380}$) with Northern Eclipse Image software (Empix Imaging, Inc., Mississauga, ON, Canada). Fluorescence ratios ($F_{340}/F_{380}$) were converted to an absolute $[Ca^{2+}]_i$ concentration using the equation of $[Ca^{2+}]_i = K_d(F_{min}/F_{max})[(R - R_{min})/(R_{max} - R)]$, where $K_d$ is the dissociation constant of fura-2, $F$ is the emitted fluorescence from 380 nm excitation, and $R$ is the fluorescence ratio. The $K_d$ for fura-2 was taken to be 135 nM at room temperature. A correction factor of 0.85 was used to account for the increased viscosity of the intracellular milieu. Values for $F_{min}$ and $R_{min}$ were determined by measuring fluorescence of a 1 $\mu$M solution of fura-2 pentapotassium salt in a cell- and $Ca^{2+}$-free calibration solution (140 mM KCl, 10 mM NaCl, 10 mM HEPES, and 1 mM EGTA, pH 7.2); background fluorescence was determined in calibration solution before the addition of fura-2. Values for $F_{max}$ and $R_{max}$ were determined after the addition of a saturating amount of $CaCl_2$ (1 mM).

**Drug Treatments.** All drugs were freshly dissolved in 1× PBS with or without an aid of dimethyl sulfoxide (DMSO) and warmed to 37°C in the incubator before being directly applied onto cultures. Whenever DMSO was used, PBS containing the same concentration of DMSO was used as control vehicle. DHPG, *N*-phenyl-7-(hydroxyimino)cyclopropa[b]chromen-1*a*-carboxamide (PHCCC), (*R*,*S*)-*α*-methylserine-*O*-phosphate monophenyl ester (MSOPPE), 7-(hydroxyimino)cyclopropa[b]chromen-1*a*-carboxylate ethyl ester (CPCCOet), 2-methyl-6-(phenylethynyl)pyridine hydrochloride (MPEP), NMDA, AMPA, (+)-MK801, DL-2-amino-5-phosphonovaleric acid (AP5), DNQX, verapamil hydrochloride, nifedipine, ryanodine, and thapsigargin were purchased from Tocris Cookson Inc. (Ballwin, MO). U73122, U73343, and xestospongin C were purchased from Calbiochem (San Diego, CA). The L-type $Ca^{2+}$ channel activator 2,5-dimethyl-4-[2-(phenylmethyl)benzoyl]-1*H*-pyrrole-3-carboxylic acid methylester (FPL64176) was purchased from Sigma-Aldrich.

**Statistics.** The results are presented as mean ± S.E.M. The percentages of pCREB-positive cells and $Ca^{2+}$ levels were evaluated using a one- or two-way analysis of variance, as appropriate, followed by a Bonferroni (Dunn) comparison of groups using least-squares-adjusted means. Probability levels of $<0.05$ were considered statistically significant.

## Results

**Effects of DHPG on CREB Phosphorylation.** This first study tested whether DHPG stimulation of group I mGluRs alters CREB phosphorylation in cultured striatal neurons. We found that DHPG incubation (10 min) at different concentrations caused concentration-dependent increases in pCREB immunoreactivity. In the culture treated with a control vehicle, very few pCREB-positive cells were exhibited (Fig. 1A). DHPG at its lower concentration range (0.16–4 $\mu$M) did not cause significant changes in the number of pCREB-immunoreactive cells (data not shown). At 20 $\mu$M, DHPG started to induce a reliable increase in the percentage of pCREB-labeled cells (Fig. 1B). Two higher concentrations (50 and 100 $\mu$M) induced greater increases in pCREB cells (Fig. 1C). DHPG at 500 $\mu$M caused an increase in pCREB cells no greater than that induced by 100 $\mu$M (Fig. 1D). The pCREB immunoreactivity was confined to the nucleus of perikarya, and no specific immunostaining was seen in the neural processes and cytoplasms (Fig. 1E). The basal and increased pCREB primarily occurred in the medium-sized neurons. In contrast, glial cells, mainly astrocytes, did not show detectable pCREB staining under both normal and DHPG-treated conditions. Fig. 1K shows the results from the quantitation in

terms of percent changes in the number of pCREB cells after DHPG treatments.

To profile temporal properties of the pCREB induction, 100 $\mu$M DHPG, which produced a maximal pCREB immunostaining in the dose-response study mentioned above, was added to the cultures for different periods of incubation. As shown in Fig. 1, F through J and L, significant pCREB induction was evident after a 3-min treatment. The increased pCREB cells peaked during 10 to 15 min of incubation and gradually declined to the basal level by 6 h. Based on these time-response and above-mentioned dose-response effects, DHPG was therefore incubated at 100 $\mu$M for 10 min in all following experiments for dissecting mechanisms underlying DHPG-stimulated CREB phosphorylation at receptor and signaling protein levels.

Upon the demonstration of a marked increase in pCREB cells, the phenotype of these cells was examined using double immunofluorescent labeling on cultures exposed to 100 $\mu$M DHPG for 10 min. Almost all of the pCREB cells showed coimmunostaining for the neuronal marker MAP2 (Fig. 2, A-D) in their cytoplasms and processes and for another neuronal marker, NeuN, in their nuclei (Fig. 2, E-H). Moreover, all pCREB-positive cells were associated with GABA immunoreactivity in cytoplasmic compartments (Fig. 2, I-L). Thus, the CREB phosphorylation predominantly occurred in GABA-ergic neuronal cells.

To probe the effect of DHPG on basal levels of CREB immunoreactivity in striatal neurons, three concentrations of DHPG (0.8, 20, and 100 $\mu$M) were incubated for 10 or 30 min. None of the drug treatments had significant effects on the number and density of CREB-immunoreactive neurons (Fig. 3).

**Effects of the Group I or II/III Antagonist on DHPG-Stimulated CREB Phosphorylation.** To determine whether DHPG-stimulated CREB phosphorylation is a group I receptor-mediated event, the group I antagonist PHCCC

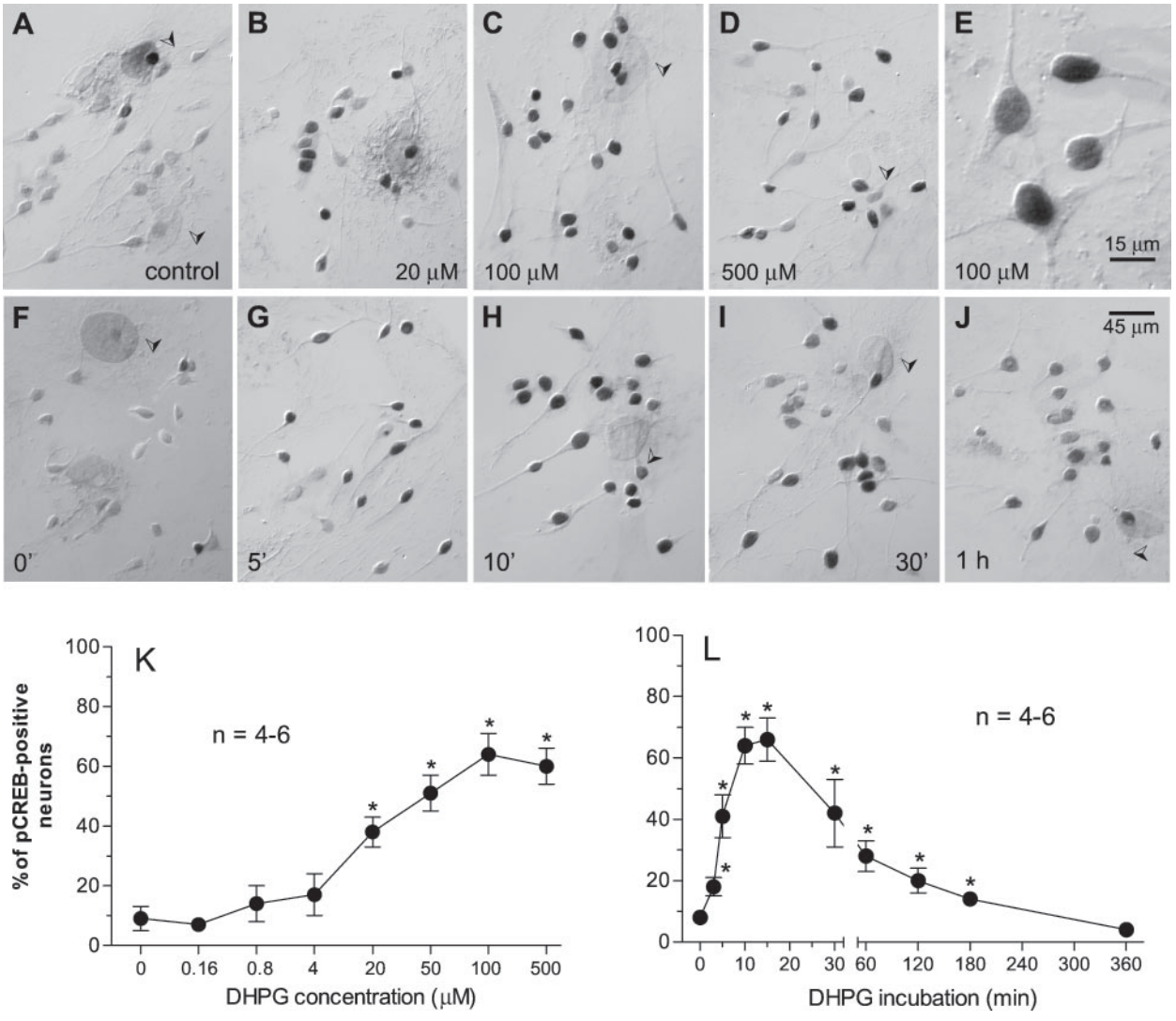


**Fig. 1.** Dose- and time-dependent increases in CREB phosphorylation in rat primary cultures of striatal neurons after incubation of the group I mGluR agonist DHPG. The number of pCREB-immunoreactive neurons was increased after 10-min incubation of DHPG at concentrations ranging from 0.16 to 500 $\mu$M in a concentration-dependent manner (A through D and K). The increased pCREB immunostaining was exclusively expressed within the nuclear compartment (E). F through J and L show the temporal alterations in the number of pCREB-immunoreactive neurons after incubation of 100 $\mu$M DHPG for 2 min to 6 h. The DHPG-stimulated CREB phosphorylation occurred in the medium-sized neuronal cells rather than the astroglial cells with large, flat and phase-dark nuclei (arrows). Data are the mean ± S.E.M. of the percentage change in numbers of the pCREB-positive cells from four to six wells (K and L). $\star$ $p < 0.05$ compared with control.

was coincubated with DHPG (100 $\mu$M) for 10 min. Although PHCCC at 2 $\mu$M did not alter DHPG-stimulated pCREB, PHCCC at 10 $\mu$M largely reduced the pCREB-positive neurons (Fig. 4I). In the presence of 50 $\mu$M PHCCC, DHPG completely lost its ability to increase pCREB cells (Fig. 4, C versus D). To investigate the effects of PHCCC on basal pCREB expression, PHCCC was incubated alone for 10 min. Although PHCCC at three concentrations tended to decrease basal levels of pCREB, they did not reach statistically significant levels (Fig. 4I). Effects of the group II/III antagonist

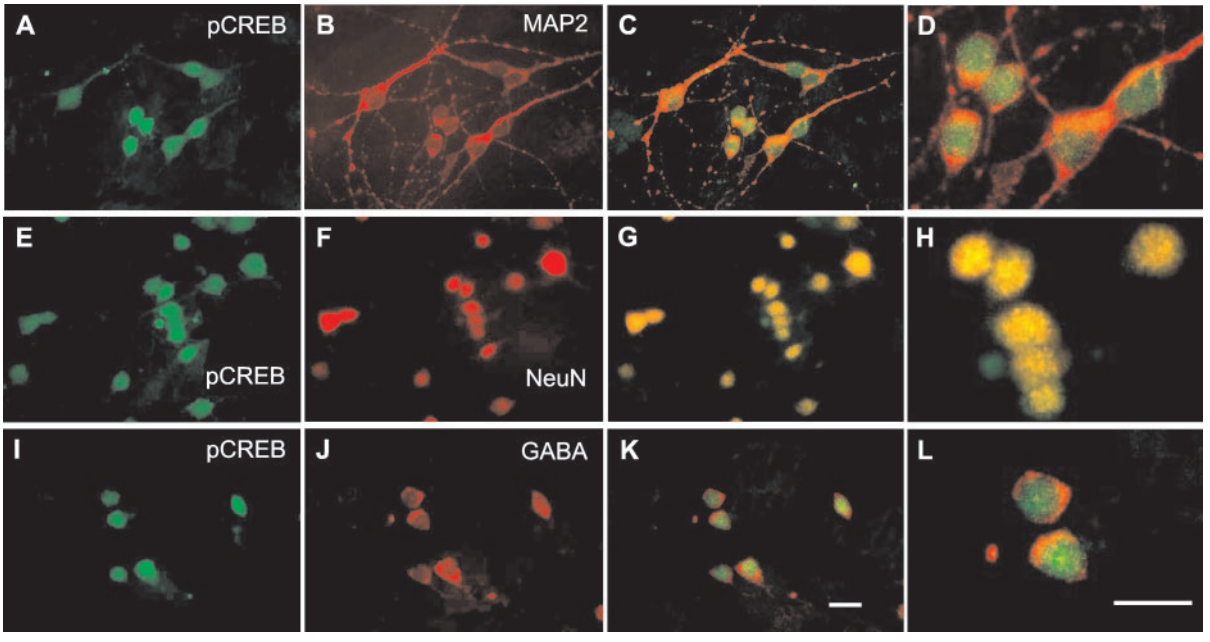


**Fig. 2.** Fluorescent microscope images showing phenotypic characterizations of pCREB-positive cells in cultured striatal neurons. Double immunofluorescent labeling for pCREB (green; A, E, and I) with MAP2 (red; B), NeuN (red; F) or GABA (red; J) was performed in cultures exposed to 100 $\mu$M DHPG for 10 min. All pCREB-positive cells are colocalized with MAP2 (yellow; C and D), NeuN (yellow; G and H), or GABA (yellow; K and L). Scales (K and L) = 20 $\mu$M.

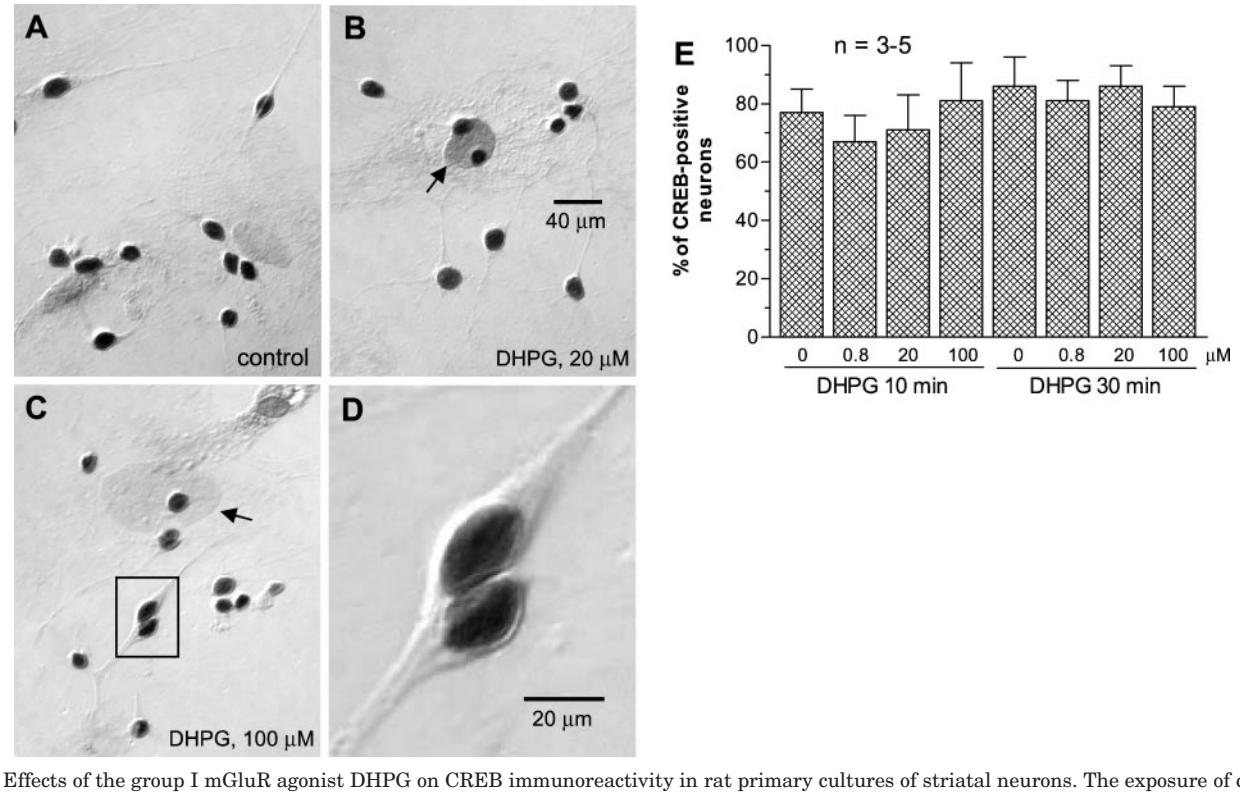


**Fig. 3.** Effects of the group I mGluR agonist DHPG on CREB immunoreactivity in rat primary cultures of striatal neurons. The exposure of cultures to DHPG (0.8 to 100 $\mu$M for 10 or 30 min) did not alter the number and density of CREB-immunoreactive neurons (A-C and E). At a magnified view, CREB staining was localized in the nuclear compartment (D). Data are the mean ± S.E.M. of the percentage change in numbers of the CREB-positive neurons from three to five wells (E).

MSOPPE on basal and DHPG-stimulated CREB phosphorylation were also assessed in a separate experiment, and the results are illustrated in Fig. 4, E through H and J. Unlike PHCCC, MSOPPE at the equimolar concentrations (2, 10, and 50 $\mu$M for 10 min alone or with 100 $\mu$M DHPG) showed no significant effects on both constitutive and DHPG-stimulated pCREB expression.

**Effects of the mGluR1 or 5 Antagonist on DHPG-Stimulated CREB Phosphorylation.** To evaluate the relative importance of mGluR1 and 5, an mGluR1 or mGluR5 antagonist (CPCCOet for mGluR1 and MPEP for mGluR5) was coincubated with 100 $\mu$M DHPG for 10 min. The mGluR1 antagonist CPCCOet did not alter DHPG-stimulated pCREB at all three concentrations surveyed (Fig. 5A). In contrast, MPEP attenuated the DHPG-stimulated pCREB expression in a concentration-dependent manner (Fig. 5B). Neither CPCCOet nor MPEP altered basal pCREB expression (Fig. 5).

**Effects of the NMDA or Kainate/AMPA Antagonist on DHPG-Stimulated CREB Phosphorylation.** To evaluate the participation of NMDA and kainate/AMPA receptors in the DHPG action, effects of coincubation of the NMDA antagonist MK801 (noncompetitive) or AP5 (competitive) or the kainate/AMPA antagonist DNQX with DHPG (100 $\mu$M for 10 min) on DHPG-stimulated pCREB were examined in cultured striatal neurons. MK801 at 0.1 and 1 $\mu$M caused a partial and complete blockade of NMDA-stimulated pCREB expression, respectively (Fig. 6A). Both concentrations of MK801 also partially attenuated pCREB induction by DHPG (Fig. 6A). AP5 at 50 but not 5 $\mu$M induced a complete and partial blockade of NMDA- and DHPG-induced pCREB cells, respectively (Fig. 6B). Unlike the NMDA antagonists, DNQX (10 or 100 $\mu$M) had no significant effects on DHPG-induced pCREB expression, although it blocked pCREB induction by 50 $\mu$M AMPA (Fig. 6C). Blockade of both NMDA and non-NMDA receptors was also attempted by giving MK801 and DNQX at the same time (Fig. 6D). Still, the partial inhibition of DHPG-stimulated pCREB cells was seen in the presence of MK801 and DNQX (Fig. 6D). None of the three antagonists affected basal pCREB expression when given alone.

**Effects of the L-Type VOCC Blockers on DHPG-Stimulated CREB Phosphorylation.** To evaluate whether the L-type VOCCs contribute to DHPG-stimulated pCREB expression, the two L-type VOCC blockers (nifedipine and verapamil) were coincubated with DHPG for 10 min. Nifedipine at 20 but not 2 $\mu$M completely eliminated pCREB induction

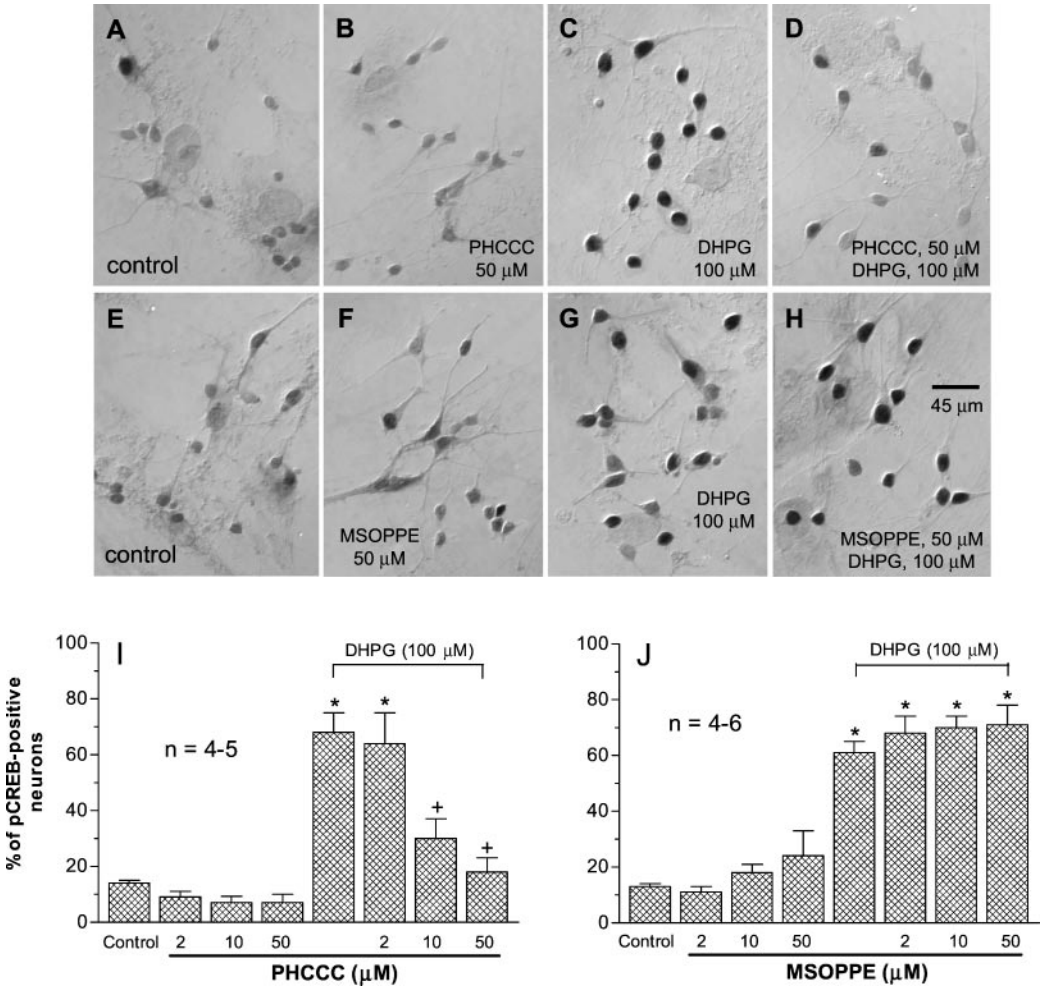


**Fig. 4.** Effects of the mGluR subgroup-selective antagonists on basal and the group I mGluR agonist DHPG-stimulated pCREB immunoreactivity in rat primary cultures of striatal neurons. The group I antagonist PHCCC did not affect basal pCREB expression but concentration-dependently blocked DHPG-induced increases in the number of pCREB neurons (A-D and I). The group II/III antagonist MSOPPE had no significant effects on basal and DHPG-stimulated pCREB expression (E-H and J). Data are the mean ± S.E.M. of the percentage change in numbers of the pCREB-positive neurons from four to six wells (I and J). ⋆, $p < 0.05$ compared with control and +, $p < 0.05$ compared with 100 $\mu$M DHPG.

induced by the L-type VOCC activator FPL64176 (20 μM; Fig. 7A). The drug at 20 μM also substantially attenuated DHPG-induced increases in pCREB cells (Fig. 7A). Verapamil produced the results parallel with those induced by nifedipine (Fig. 7B). The ability of DHPG to stimulate pCREB expression was also tested in the extracellular $Ca^{2+}$-free solution. In the absence of $Ca^{2+}$, DHPG no longer induced a significant increase in pCREB cells (Fig. 7C versus Fig. 1K), indicating the dependence of DHPG effect on the presence of extracellular $Ca^{2+}$ ions.

**CREB Phosphorylation Induced by NMDA or L-Type VOCC Activation.** The studies were pursued to evaluate the interactions among NMDA receptors, L-type VOCCs, and group I mGluRs in facilitating CREB phosphorylation. NMDA-induced (50 μM) increases in pCREB neurons were blocked by 1 μM MK801 but not by 50 μM PHCCC or 20 μM nifedipine (Fig. 8A). Thapsigargin (1 μM for 1 h before and during 10-min NMDA incubation), an agent that depletes internal $Ca^{2+}$ stores, did not affect the NMDA action (Fig. 8A). Similarly, FPL64176-induced (20 μM) pCREB expression was blocked by nifedipine but not by MK801, PHCCC, or thapsigargin (Fig. 8B).

**Role of PLC Activation and Intracellular $Ca^{2+}$ Release in DHPG-Stimulated CREB Phosphorylation.**

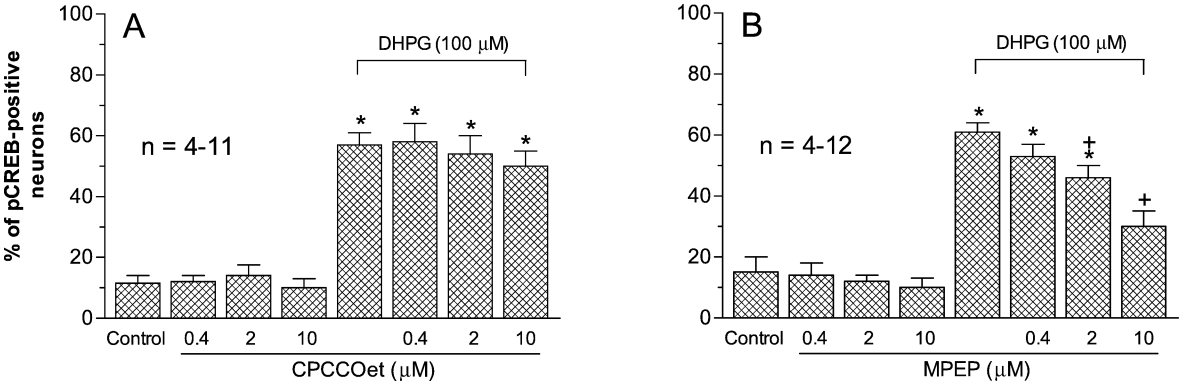


**Fig. 5.** Effects of the mGluR1 antagonist CPCCOet (A) or mGluR5 antagonist MPEP (B) on basal and the group I mGluR agonist DHPG-stimulated pCREB immunoreactivity in rat primary cultures of striatal neurons. Data are the mean ± S.E.M. of the percentage change in numbers of the pCREB-positive neurons. ⋆, $p < 0.05$ compared with control and +, $p < 0.05$ compared with 100 μM DHPG.

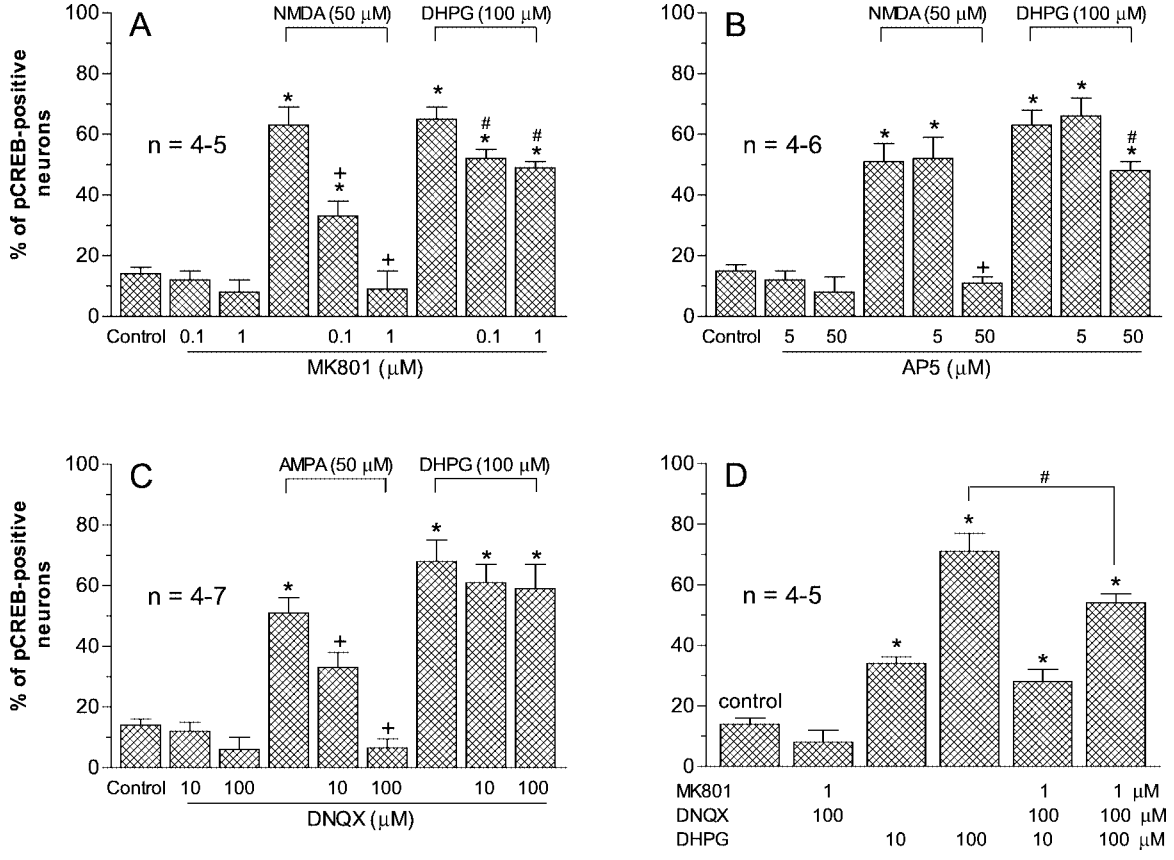


**Fig. 6.** Effects of the ionotropic glutamate receptor antagonists on the group I mGluR agonist DHPG-stimulated pCREB immunoreactivity in rat primary cultures of striatal neurons. MK801 (A), AP5 (B), DNQX (C), or MK801+DNQX (D) was coadministered with DHPG for 10 min. Data are the mean ± S.E.M. of the percentage change in numbers of the pCREB-positive neurons from four to seven wells. ⋆, $p < 0.05$ compared with control; +, $p < 0.05$ compared with 50 μM NMDA (A and B) or 50 μM AMPA (C); and #, $p < 0.05$ compared with 100 μM DHPG.

Group I mGluRs are positively coupled to the PLC. To determine the PLC involvement in DHPG-stimulated pCREB, the PLC inhibitor U73122 or its inactive analogue U73343 was coincubated with DHPG (100 $\mu$M) for 10 min. From Fig. 9A, U73122 attenuated DHPG-induced increases in pCREB neurons in a concentration-dependent manner. In contrast, U73343 at all three concentrations (2.5, 10, and 40 $\mu$M) had no effects on the DHPG phosphorylation of CREB (data not shown). To determine whether $IP_3$ or ryanodine receptors, which are both localized on internal $Ca^{2+}$ stores in striatal neurons (Martone et al., 1997) and process evoked $[Ca^{2+}]_i$ release, mediate the DHPG effect, the cell-permeable inhibitor for either $IP_3$ (xestospongin C) or ryanodine receptors was coincubated with DHPG (10 min). DHPG-stimulated CREB phosphorylation was blocked by xestospongin C at the two higher concentrations (1 and 4 $\mu$M; Fig. 9B) but not by ryanodine at any concentration (Fig. 9C). Finally, the $[Ca^{2+}]_i$-depleting agent thapsigargin (for 1 h before and during 10-min DHPG treatment) blocked the DHPG induction of pCREB neurons in a concentration-dependent manner (Fig. 9D).

**$[Ca^{2+}]_i$ Imaging and Ratiometric Measurements of Cytoplasmic Free $Ca^{2+}$ Concentrations.** $[Ca^{2+}]_i$ levels were measured using fura-2 at a single neuron level to examine how intracellular $Ca^{2+}$ signals are modified by intracellular mobilization and influx. DHPG (100 $\mu$M) consistently induced a rapid and transient $[Ca^{2+}]_i$ rise in neurons, which was followed by a progressively larger increase in $[Ca^{2+}]_i$ (Fig. 10A). In the absence of extracellular $Ca^{2+}$ ions, 100 $\mu$M DHPG induced only an initial $[Ca^{2+}]_i$ rise (Fig. 10B), indicating that the initial and delayed phases of $[Ca^{2+}]_i$ rises were independent and dependent of extracellular $Ca^{2+}$, respectively. In the presence of xestospongin C (1 $\mu$M), DHPG did not significantly alter $[Ca^{2+}]_i$ levels throughout the course (Fig. 10C). Blockade of $Ca^{2+}$-permeable NMDA receptors with MK801 (1 $\mu$M) did not affect the DHPG-induced transient $[Ca^{2+}]_i$ rise but slightly reduced the second $Ca^{2+}$ response (Fig. 10, D and F). Blockade of L-type VOCCs with nifedipine (20 $\mu$M) greatly attenuated the late $Ca^{2+}$ response without altering the early $[Ca^{2+}]_i$ rise (Fig. 10, E and F). An example illustrating dynamic changes in $[Ca^{2+}]_i$ fluorescent images in response to 100 $\mu$M DHPG stimulation is shown in Fig. 10, G through J.

To evaluate developmental conditions of cultured striatal neurons in their capability of responding to group I receptor stimulation in terms of the $[Ca^{2+}]_i$ rise and CREB phosphorylation, DHPG effects were surveyed after different days in culture. The numbers of responsive neurons displaying the significant $[Ca^{2+}]_i$ rise and pCREB induction showed a steady increase along increased days in culture after DHPG

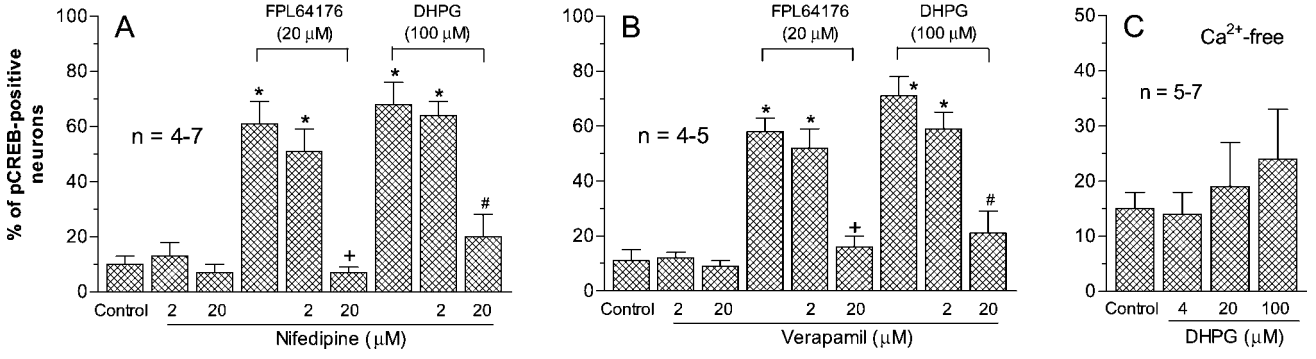


**Fig. 7.** Effects of the L-type VOCC blockers on the DHPG-stimulated pCREB immunoreactivity in rat primary cultures of striatal neurons. The selective L-type VOCC blocker, nifedipine (A) or verapamil (B), was coadministered with DHPG for 10 min. Data are the mean ± S.E.M. of the percentage change in numbers of the pCREB-positive neurons from four to seven wells. ⋆, $p < 0.05$ compared with control; +, $p < 0.05$ compared with 20 $\mu$M FPL64176; and #, $p < 0.05$ compared with 100 $\mu$M DHPG. C, effects of DHPG (10 min) on numbers of pCREB neurons in $Ca^{2+}$-free solution.

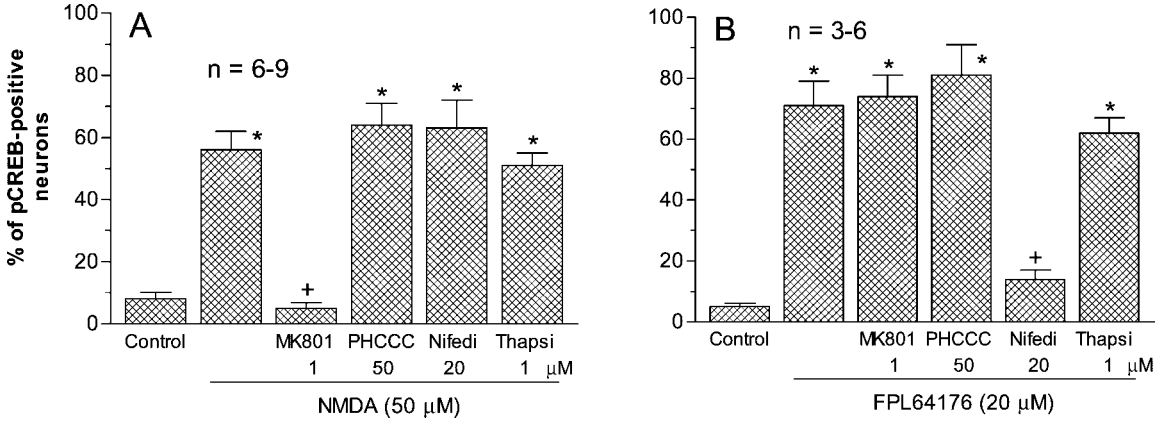


**Fig. 8.** Induction of pCREB immunoreactivity in rat primary cultures of striatal neurons after activation of NMDA receptors (A) and L-type VOCCs (B). NMDA or FPL64176 was applied alone or with one of three antagonists (MK801, PHCCC, or nifedipine) for 10 min. Thapsigargin was applied 1 h before and during 10 min NMDA or FPL64176 incubation. Data are the mean ± S.E.M. of the percentage change in numbers of the pCREB-positive neurons from three to nine wells. ⋆, $p < 0.05$ compared with control and +, $p < 0.05$ compared with 50 $\mu$M NMDA (A) or 20 $\mu$M FPL64176 (B).

application (Fig. 10K). The maximal levels were reached between 15 and 20 days (Fig. 10K).

## Discussion

The present study examined CREB phosphorylation in response to group I mGluR stimulation. We found that the group I agonist DHPG increased pCREB levels in cultured striatal neurons in concentration- and time-dependent manners. The pCREB induction occurred in GABA-ergic neurons but not glia. Blockade of group I but not II/III mGluRs abolished the CREB phosphorylation. Moreover, blockade of mGluR5 but not mGluR1 attenuated the DHPG effect. Interestingly, the L-type VOCC inhibitors also blocked DHPG-stimulated pCREB immunoreactivity. Prolonged incubation of DHPG induced a rapid and transient $Ca^{2+}$ release, which was sensitive to the $IP_3$ receptor inhibitor. The transient $Ca^{2+}$ release was followed by a progressively larger rise in $[Ca^{2+}]_i$ via the L-type VOCC- and NMDA-mediated $Ca^{2+}$ influx, which is responsible for the concurrent CREB phosphorylation. These results demonstrated an effective signaling pathway from mGluR5 to $Ca^{2+}$ signals resulting in CREB phosphorylation.

The CREB phosphorylation induced by DHPG was characterized in several aspects. First, the phosphorylation responses were dose- and time-dependent. The time course of the dynamic phosphorylation generally resembles that observed after dopamine or ionotropic glutamate receptor stimulation or L-type VOCC activation via KCl depolarization in striatal neurons both in vivo (Cole et al., 1995; Choe and McGinty, 2000) and in vitro (Das et al., 1997; Liu and Graybiel, 1998; Rajadhyaksha et al., 1999; Macias et al., 2001). Second, the CREB phosphorylation predominantly occurred in medium-sized neuronal cells but not glia. Because all pCREB-immunoreactive neurons showed coexpression with GABA, the CREB phosphorylation is believed to take place in GABA-ergic neurons, the phenotype of projection neurons in the striatum representing 95% of a total population of striatal cells. The anatomical data that group I mGluRs (especially mGluR5 subtypes) are densely distributed in projection neurons (Fotuhi et al., 1993; Shigemoto et al., 1993; Testa et al., 1995; Kerner et al., 1997; Tallaksen-Greene et al., 1998) supports the occurrence of the CREB phosphorylation mainly in GABA-ergic neurons. Third, no significant alteration in basal levels of CREB immunoreactivity was seen after DHPG treatments. This is in agreement with the notion that pCREB levels were increased via its phosphorylation on $Ser^{133}$ but not via an increase in its protein levels (Konradi et al., 1994; Rajadhyaksha et al., 1999). And last, DHPG-induced pCREB was blocked by a group I antagonist, PHCCC, but not by a group II/III antagonist, MSOPPE. Our previous studies have validated the potency and selectivity of PHCCC in blocking group I receptors (Wang and Mao, 2000; Mao and Wang, 2001a,b). The PHCCC blockade of the DHPG action in the present study indicates a PHCCC-sensitive group I receptor mechanism in mediating the DHPG phosphorylation of CREB. In a further effort to

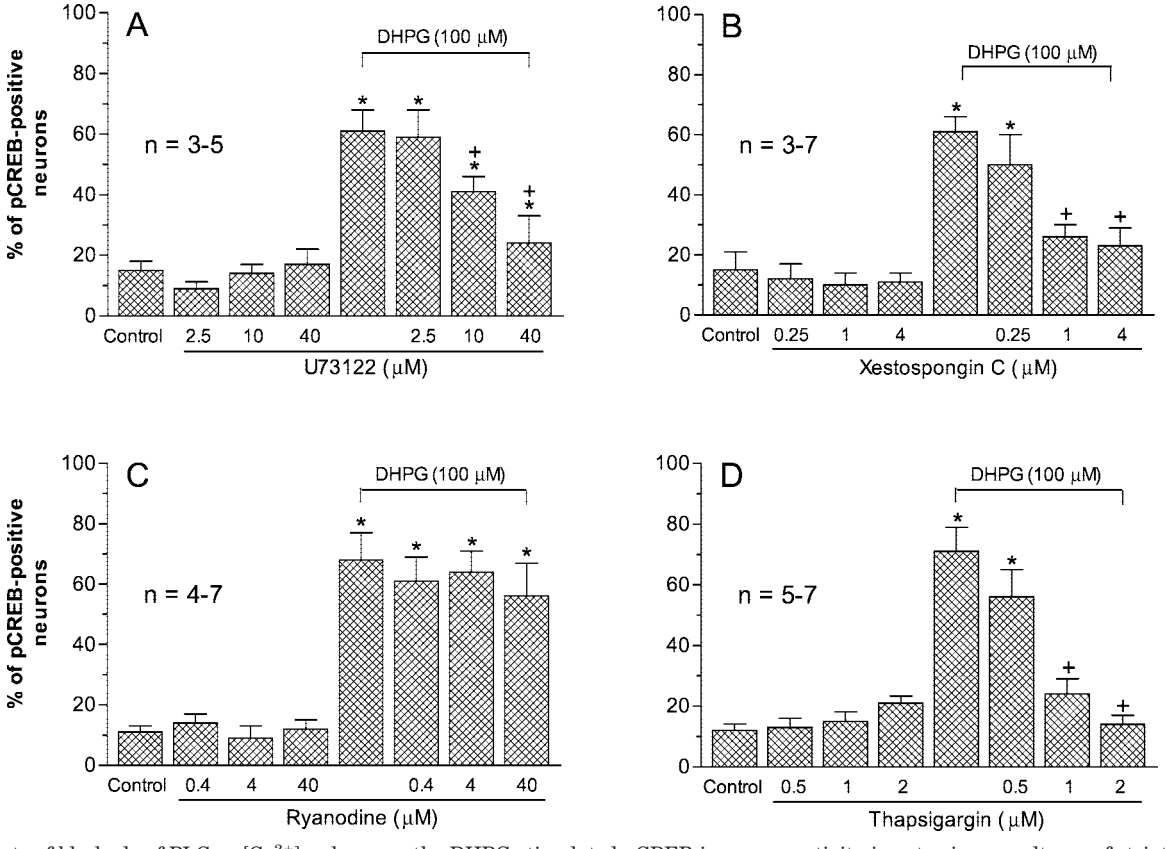


**Fig. 9.** Effects of blockade of PLC or $[Ca^{2+}]_i$ release on the DHPG-stimulated pCREB immunoreactivity in rat primary cultures of striatal neurons. The PLC inhibitor U73122 (A) or the $[Ca^{2+}]_i$ release inhibitor xestospongin C (B) or ryanodine (C) was coadministered with DHPG for 10 min. Thapsigargin was applied 1 h before and during 10-min DHPG incubation (D). Data are the mean ± S.E.M. of the percentage change in numbers of the pCREB-positive neurons from three to seven wells. ⋆, $p < 0.05$ compared with control and +, $p < 0.05$ compared with 100 μM DHPG.

clarify the relative importance of mGluR1 and 5 subtypes, we found that the DHPG effect was much more sensitive to the mGluR5 antagonist than the mGluR1 antagonist. Apparently, selective activation of mGluR5 rather than mGluR1 mediates the DHPG action.

A series of pharmacological studies was carried out to dissect signaling steps toward CREB phosphorylation. An initial postreceptor step involves activation of the receptor-bound PLC, because the PLC inhibitor U73122 eliminated the DHPG-induced CREB phosphorylation. Group I receptor/PLC then sequentially stimulates phosphoinositide turnover to give rise to $IP_3$, which interacts with $IP_3$ receptors on $Ca^{2+}$ stores to cause $Ca^{2+}$ release. This was demonstrated by the finding that inhibition of $IP_3$ receptors with xestospongin C blocked the DHPG effect. The importance of $Ca^{2+}$ release was further confirmed by the blocking effect of the $Ca^{2+}$-depleting agent thapsigargin. In contrast to $IP_3$ receptors, another family of $Ca^{2+}$ release channels, ryanodine-sensitive channels, which are expressed in striatal neurons like $IP_3$ receptors (Martone et al., 1997), may not be significantly linked to the $Ca^{2+}$ release, because ryanodine at a high dose did not affect the DHPG effect. It seems that PLC and $IP_3$ constitute the key transducers to process group I-sensitive $Ca^{2+}$ mobilization. Interestingly, in addition to $Ca^{2+}$ release, $Ca^{2+}$ influx was revealed as an essential link in the biocascade to CREB phosphorylation, because the inhibition of L-type VOCCs almost totally blocked the DHPG-phosphorylated CREB.

The relationship of $Ca^{2+}$ release and influx was then examined using ratiometric $Ca^{2+}$ imaging. Prolonged DHPG incubation induced a rapid and transient $Ca^{2+}$ rise followed by a delayed and progressive increase in $Ca^{2+}$ levels. These biphasic responses are in good accordance with those observed in hippocampal or cortical neurons in response to DHPG exposure (Prothero et al., 1998; Bianchi et al., 1999) or activation of other metabotropic receptors, such as muscarinic and purinergic receptors (Bouron, 2000; Prothero et al., 2000; Grimaldi et al., 2001). The initial $Ca^{2+}$ rise is appar-

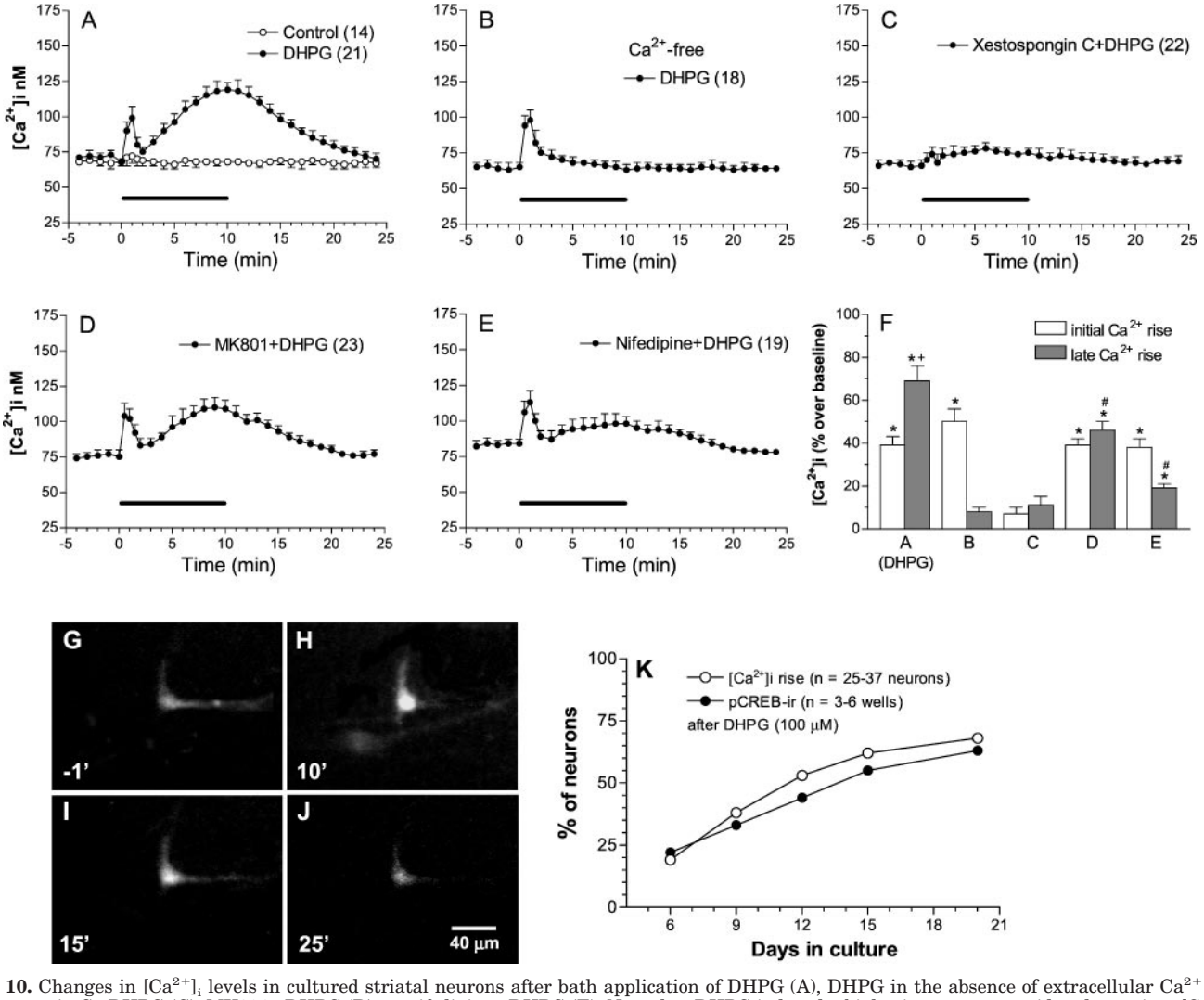


**Fig. 10.** Changes in $[Ca^{2+}]_i$ levels in cultured striatal neurons after bath application of DHPG (A), DHPG in the absence of extracellular $Ca^{2+}$ (B), xestospongin C+DHPG (C), MK801+DHPG (D), or nifedipine+DHPG (E). Note that DHPG induced a biphasic response: rapid and transient $[Ca^{2+}]_i$ rise followed by a progressively larger $[Ca^{2+}]_i$ increase (A). The horizontal bars (A-E) represent duration of drug applications (10 min). A bar graph represents data from A through E in terms of maximal changes above baselines for both initial and second $[Ca^{2+}]_i$ rises (F). ⋆, $p < 0.05$ compared with baseline; +, $p < 0.05$ as the initial $Ca^{2+}$ rise; and #, $p < 0.05$ compared with the late $Ca^{2+}$ rise induced by DHGP alone. G through J, representative recordings of DHPG-evoked $[Ca^{2+}]_i$ elevation in somatic fura-2 ratio fluorescence in a responsive neuron. Images were recorded 1 min before (G) and 10 (H), 15 (I), and 25 (J) min after DHPG application at 100 $\mu$M. K, the percentage of neurons showing a significant $[Ca^{2+}]_i$ rise or pCREB-immunoreactivity after DHPG (100 $\mu$M) treatments at different days in culture.

ently mediated by $Ca^{2+}$ release via $IP_3$-sensitive channels, because the $IP_3$ receptor inhibitor xestospongin C blocked it, and it was preserved in extracellular $Ca^{2+}$-free solution (present study; Prothero et al., 1998; Bianchi et al., 1999). The second $Ca^{2+}$ response with slower kinetics, however, was due to $Ca^{2+}$ influx, as it was eliminated in the absence of extracellular $Ca^{2+}$ ions (present study; Prothero et al., 1998; Bianchi et al., 1999). The $Ca^{2+}$ release-induced $Ca^{2+}$ influx may be largely processed by the opening of L-type VOCCs because 1) group I stimulation did cause membrane depolarization in a large number of studies (Congar et al., 1997; Bianchi et al., 1999), 2) the second phase of $Ca^{2+}$ rises appeared when depolarization reached threshold for voltage-gated $Ca^{2+}$ influx and disappeared when member potential was hyperpolarized (Bianchi et al., 1999), and 3) blockade of L-type VOCCs substantially attenuated the late $Ca^{2+}$ response (Rae et al., 2000; present study). In addition, NMDA receptors may contribute to store-operated $Ca^{2+}$ entry, although on a much lesser scale. The $Ca^{2+}$ influx was triggered to refill $Ca^{2+}$ stores in an event known as capacitative $Ca^{2+}$ entry (Prothero et al., 1998; Rae et al., 2000). More importantly, as demonstrated in the present study, evoked $Ca^{2+}$ entry can participate in the transmission of extracellular signals originated from prolonged receptor stimulation to transcriptional activity to organize an integral response (plasticity) to the circumstance.

Direct stimulation of $Ca^{2+}$-permeable NMDA receptors caused CREB phosphorylation in many cell lines and neurons. An NMDA component mediating the DHPG phosphorylation of CREB was also demonstrated in the present study, because the NMDA antagonist partially attenuated the phosphorylation response. However, NMDA receptors contribute to the CREB phosphorylation to a lesser extent compared with L-type VOCCs. Although the NMDA antagonist did not affect the initial $Ca^{2+}$ release by DHPG, a small fraction of the late $Ca^{2+}$ response was attenuated, indicating a limited NMDA element in the late event. How group I mGluRs potentiate NMDA $Ca^{2+}$ influx is unclear. It can be only assumed, according to available data, that the signals, $Ca^{2+}$ and/or diacylglycerol-protein kinase C downstream to group I stimulation, may positively interact with NMDA receptors to allow larger $Ca^{2+}$ influx, which adds to the $Ca^{2+}$ response to DHPG (Krieger et al., 2000; Skeberdis et al., 2001). Long opening times of NMDA $Ca^{2+}$ channels seem to particularly support the NMDA participation in the delayed and sustained $Ca^{2+}$ response (Ascher and Nowak, 1987; Gasic and Hollmann, 1992).

NMDA and L-type VOCCs both result in $Ca^{2+}$ influx and contribute to the DHPG effect (present study). Depending on spatiotemporal properties, NMDA- and VOCC-induced $Ca^{2+}$ influx may either cooperatively or independently regulate CREB phosphorylation (Ginty, 1997). In cultured hippocampal neurons, NMDA receptors and L-type VOCCs increased pCREB levels through independent, parallel pathways rather than to the same pathway (Bading et al., 1993, 1995). This is also the case in striatal cultures in the present study, given that the NMDA and VOCC antagonists did not affect the pCREB induction induced by the VOCC activator and NMDA, respectively. However, in striatal cells cultured for 6 to 8 days, immunoblot showed attenuation of NMDA-induced pCREB by L-type VOCC antagonists (Rajadhyaksha et al., 1999), indicating a L-type VOCC dependency of NMDA-stimulated pCREB activity. Perhaps a longer growth time of striatal neurons in the present study (15–18 days) allows the development of independent NMDA and VOCC pathways to modulate $Ca^{2+}$ influx and CREB phosphorylation.

The role of pCREB in up-regulating the transcription of genes that contain the $Ca^{2+}$ and cAMP response element site(s) in their promoter regions has been extensively studied in the central nervous system recently. In striatal neurons, pCREB has been documented to process immediate early gene c-*fos* and opioid peptide gene expression in response to dopamine receptor stimulation (Konradi et al., 1994; Cole et al., 1995). Our recent data show that the mGluR agonist ACPD increased c-*fos* and opioid peptide mRNA expression in striatal neurons (Wang, 1998; Wang and McGinty, 1998). Similarly, DHPG elevated opioid gene expression in vivo (Mao and Wang, 2001a) and in vitro (Mao and Wang, 2001b). The present study revealed a strong, positive linkage between group I receptors and CREB phosphorylation. Thus, pCREB is considered to serve as a key factor at the transcriptional level to bridge group I-regulated gene expression.





## References


Ascher P and Nowak L (1987) Electrophysiological studies of NMDA receptors. *Trends Neurosci* **10:**284–287.

Bading H, Ginty DD, and Greenberg ME (1993) Regulation of gene expression in hippocampal neurons by distinct calcium signaling pathways. *Science (Wash DC)* **260:**181–186.

Bading H, Segal MM, Sucher NJ, Dudek H, Lipton SA, and Greenberg ME (1995) *N*-methyl-D-aspartate receptors are critical for mediating the effects of glutamate on intracellular calcium concentration and immediate early gene expression in cultured hippocampal neurons. *Neuroscience* **64:**653–664.

Berridge MJ (1993) Inositol triphosphate and calcium signaling. *Nature (Lond)* **361:**315–325.

Bianchi R, Young SR, and Wong RKS (1999) Group I mGluR activation causes voltage-dependent and -independent $Ca^{2+}$ rises in hippocampal pyramidal cells. *J Neurosci* **81:**2903–2913.

Bito H, Deisseroth K, and Tsien RW (1996) CREB phosphorylation and dephosphorylation: a $Ca^{2+}$-and stimulus duration-dependent switch for hippocampal gene expression. *Cell* **87:**1203–1214.

Bordi F and Ugolini A (1999) Group I metabotropic glutamate receptors: implications for brain diseases. *Prog Neurobiol* **59:**55–79.

Bouron A (2000) Activation of a capacitative $Ca^{2+}$ entry pathway by store depletion in cultured hippocampal neurons. *FEBS Lett* **470:**269–272.

Bourtchuladze R, Frenguelli B, Blendie J, Cioffi D, Schutz G, and Silva AJ (1994) Deficient long-term memory in mice with a targeted mutation of the cAMP-response element-binding protein. *Cell* **79:**59–68.

Choe ES and McGinty JF (2000) *N*-methyl-D-aspartate receptors and p38 mitogen-activated protein kinase are required for cAMP-dependent cyclase response element binding protein and Elk-1 phosphorylation in the striatum. *Neuroscience* **101:**607–617.

Choe ES and Wang JQ (2001) Group I metabotropic glutamate receptor activation increases phosphorylation of cAMP response element-binding protein, Elk-1 and extracellular signal-regulated kinases in rat dorsal striatum. *Mol Brain Res* **94:**75–84.

Cole RL, Konradi C, Douglass J, and Hyman SE (1995) Neuronal adaptation to amphetamine and dopamine: molecular mechanisms of prodynorphin gene regulation in rat striatum. *Neuron* **14:**813–823.

Congar P, Leinekugel X, Ben-Ari Y, and Crepel V (1997) A long-lasting calcium-activated non-selective cationic current is generated by synaptic stimulation or exogenous activation of group I metabotropic glutamate receptors in CA1 pyramidal neurons. *J Neurosci* **17:**5366–5379.

Conn PJ and Pin JP (1997) Pharmacology and function of metabotropic glutamate receptors. *Annu Rev Pharmacol Toxicol* **37:**205–237.

Das S, Grunert M, Williams L, and Vincent SR (1997) NMDA and D1 receptors regulate the phosphorylation of CREB and the induction of c-fos in striatal neurons in primary culture. *Synapse* **25:**227–233.

Dolmetsch RF, Pajvani U, Spotts FK, and Greenberg ME (2001) Signaling to the nucleus by an L-type calcium channel-calmodulin complex through the MAP kinase pathway. *Science (Wash DC)* **294:**333–339.

Kearney JA, Frey KA, and Albin RL (1997) Metabotropic glutamate agonist-induced rotation: a pharmacological, Fos immunohistochemical and [$^{14}$C]-2-deoxyglucose autoradiographic study. *J Neurosci* **17:**4415–4425.

Fotuhi M, Sharp AH, Glatt CE, Hwang PM, von Krosigk M, Snyder SH, and Dawson TM (1993) Differential localization of phosphoinositide-linked metabotropic glutamate receptor (mGluR1) and the inositol 1,4,5-trisphosphate receptor in rat brain. *J Neurosci* **13:**2001–2012.

Gasic G and Hollmann M (1992) Molecular neurobiology of glutamate receptors. *Annu Rev Physiol* **54:**507–536.

Ghosh A and Greenberg ME (1995) Calcium signaling in neurons: molecular mechanisms and cellular consequences. *Science (Wash DC)* **268:**239–247.

Ginty DD (1997) Calcium regulation of gene expression: isn't that spatial? *Neuron* **18:**183–186.
Greenberg ME, Thompson MA, and Sheng M (1992) Calcium regulation of immediate early gene transcription. *J Physiol (Lond)* **86:**99–108.
Grimaldi M, Atzori M, Ray P, and Alkon DL (2001) Mobilization of calcium from intracellular stores, potentiation of neurotransmitter-induced calcium transients and capacitative calcium entry by 4-aminopyridine. *J Neurosci* **21:**3135–3143.
Hardingham GE, Arnold FJL, and Bading H (2001) A calcium microdomain near NMDA receptors: on switch for ERK-dependent synapse-to-nucleus communication. *Nat Neurosci* **4:**565–566.
Hardingham GE, Chawla S, Johnson CM, and Bading H (1997) Distinct functions of nuclear and cytoplasmic calcium in the control of gene expression. *Nature (Lond)* **385:**260–265.
Johnson CM, Hill CS, Chawla S, Treisman R, and Bading H (1997) Calcium controls gene expression via three distinct pathways that can function independently of the Ras/mitogen-activated protein kinases (ERKs) signaling cascade. *J Neurosci* **17:** 6189–6202.
Kendall DA (1993) Direct and indirect responses to metabotropic glutamate receptor activation in the brain. *Biochem Soc Trans* **21:**1120–1123.
Kerner JA, Standaert DG, Penney JB, Young AB Jr, and Landwehrmeyer GB (1997) Expression of group one metabotropic receptor subunit mRNAs in neurochemically identified neurons in the rat neostriatum, neocortex and hippocampus. *Mol Brain Res* **48:**259–269.
Konradi C, Cole RL, Heckers S, and Hyman SE (1994) Amphetamine regulates gene expression in rat striatum via transcription factor CREB. *J Neurosci* **14:**5623–5634.
Krieger P, Hellgren-Kotaleski J, Kettunen P, and El Manira AJ (2000) Interaction between metabotropic and ionotropic glutamate receptors regulates neuronal network activity. *J Neurosci* **20:**5382–5391.
Liu FC and Graybiel AM (1998) Region-dependent dynamics of cAMP response element-binding protein phosphorylation in the basal ganglia. *Proc Natl Acad Sci USA* **95:**4708–4713.
Macias W, Carlson R, Rajadhyaksha A, Barczak A, and Konradi C (2001) Potassium chloride depolarization mediates CREB phosphorylation in striatal neurons in an NMDA receptor-dependent manner. *Brain Res* **890:**222–232.
Mao L and Wang JQ (2000) Motor stimulation following bilateral injection of the group I metabotropic glutamate receptor agonist into the dorsal striatum of rats: evidence against dependence on ionotropic glutamate receptors. *Psychopharmacology* **148:**367–373.
Mao L and Wang JQ (2001a) Selective activation of group I metabotropic glutamate receptors upregulates preprodynorphin, substance P and preproenkephalin mRNA expression in rat dorsal striatum. *Synapse* **39:**82–94.
Mao L and Wang JQ (2001b) Upregulation of preprodynorphin and preproenkephalin mRNA expression by selective activation of group I metabotropic glutamate receptors in characterized primary cultures of rat striatal neurons. *Mol Brain Res* **86:**125–137.
Martone ME, Alba SA, Edelman VM, Airey JA, and Ellisman MH (1997) Distribution of inositol-1,4,5-trisphosphate and ryanodine receptors in rat neostriatum. *Brain Res* **756:**9–21.
Montminy MR, Gonzalez GA, and Yamamoto KK (1990) Regulation of cAMP-inducible genes by CREB. *Trends Neurosci* **13:**184–188.
Nakanishi S and Masu M (1994) Molecular diversity and functions of glutamate receptors. *Annu Rev Biophys Biomol Struct* **23:**319–348.
Nestler EJ, Hope BT, and Widnell KL (1993) Drug addiction: a model for the molecular basis of neural plasticity. *Neuron* **11:**995–1006.
Perkinton MS, Sihra TS, and Williams RJ (1999) $Ca^{2+}$-permeable AMPA receptors induce phosphorylation of cAMP response element-binding protein through a phosphatidylinositol 3-kinase-dependent stimulation of the mitogen-activated protein kinase signaling cascade in neurons. *J Neurosci* **19:**5861–5874.
Prothero LS, Mathie A, and Richards CD (2000) Purinergic and muscarinic receptor activation activates a common calcium entry pathway in rat neocortical neurons and glial cells. *Neuropharmacology* **39:**1768–1778.
Prothero LS, Richards CD, and Mathie A (1998) Inhibition of inorganic ions of a sustained calcium signal evoked by activation of mGluR5 receptors in rat cortical neurons and glia. *Br J Pharmacol* **125:**1551–1561.
Rae MG, Martin DJ, Collingridge GL, and Irving AJ (2000) Role of $Ca^{2+}$ stores in metabotropic L-glutamate receptor-mediated supralinear $Ca^{2+}$ signaling in rat hippocampal neurons. *J Neurosci* **20:**8628–8636.
Rajadhyaksha A, Barczak A, Macias W, Leveque JC, Lewis SE, and Konradi C (1999) L-type $Ca^{2+}$ channels are essential for glutamate-mediated CREB phosphorylation and c-fos gene expression in striatal neurons. *J Neurosci* **19:**6348–6359.
Rajadhyaksha A, Leveque J, Macias W, Barczak A, and Konradi C (1998) Molecular components of striatal plasticity: the various routes of cyclic AMP pathways. *Dev Neurosci* **20:**204–215.
Schurov IL, McNulty S, Best JD, Sloper PJ, and Hastings MH (1999) Glutamatergic induction of CREB phosphorylation and Fos expression in primary cultures of the suprachiasmatic hypothalamus in vitro is mediated by co-ordinate activity of NMDA and non-NMDA receptors. *J Neuroendocrinol* **11:**43–51.
Segal M and Murphy DD (1998) CREB activation mediates plasticity in cultured hippocampal neurons. *Neural Plast* **6:**1–7.
Shigemoto R, Nomura S, Ohishi H, Sugihara H, Nakanishi S, and Mizuno N (1993) Immunohistochemical localization of a metabotropic glutamate receptor, mGluR5, in the rat brain. *Neurosci Lett* **163:**53–57.
Silva AJ, Kogan JH, Frankland PW, and Kida S (1998) CREB and memory. *Annu Rev Neurosci* **21:**127–148.
Simpson JN, Wang JQ, and McGinty JF (1995) Repeated amphetamine administration induces a prolonged augmentation of phosphorylated cyclase response element-binding protein and Fos-regulated antigen immunoreactivity in rat striatum. *Neuroscience* **69:**441–457.
Skeberdis VA, Lan J, Opitz T, Zheng X, Bennett MV, and Zukin RS (2001) MGluR1-mediated potentiation of NMDA receptors involves a rise in intracellular calcium and activation of protein kinase C. *Neuropharmacology* **40:**856–865.
Tallaksen-Greene SJ, Kaatz KW, Romano C, and Albin RL (1998) Localization of mGluR1a-like immunoreactivity and mGluR5-like immunoreactivity in identified populations of striatal neurons. *Brain Res* **780:**210–217.
Testa CM, Standaert DG, Landwehrmeyer GB, Penney JB Jr, and Young AB (1995) Differential expression of mGluR5 metabotropic glutamate receptor mRNA by rat striatal neurons. *J Comp Neurol* **354:**241–252.
Wang JQ (1998) Regulation of immediate early gene c-*fos* and *zif/268* mRNA expression in rat striatum by metabotropic glutamate receptor. *Mol Brain Res* **57:**46–54.
Wang JQ and Mao L (1999) Pharmacological regulation of striatal gene expression by metabotropic glutamate receptors. *Zhongguo Yao Li Xue Bao* **20:**577–584.
Wang JQ and Mao L (2000) Sustained behavioral stimulation following selective activation of group I metabotropic glutamate receptors in rat striatum. *Pharmacol Biochem Behav* **65:**439–447.
Wang JQ, Mao L, and Lau YS (2002) Glutamate cascade from metabotropic glutamate receptors to gene expression in striatal neurons: implications for psychostimulant dependence and medication, in *Glutamate and Addiction* (Herman BH ed), Humana Press, New Jersey.
Wang JQ and McGinty JF (1998) Metabotropic glutamate receptor agonist increases neuropeptide mRNA expression in rat striatum. *Mol Brain Res* **54:**262–270.
Yin JC, Wallach JS, Del Vecchio M, Wilder EL, Zhou H, Quinn WG, and Tully T (1994) Induction of a dominant negative CREB transgene specifically blocks long-term memory in *Drosophila*. *Cell* **79:**49–58.

**Address correspondence to:** Dr. John Q. Wang, Department of Pharmacology, School of Pharmacy, University of Missouri-Kansas City, Kansas City, MO 64108. E-mail: wangjq@umkc.edu